THE RICH SYSTEM OF LHCb*

T. Bellunato

On behalf of the LHCb RICH Collaboration

Universitá degli Studi di Milano Bicocca and INFN
via Festa del Perdono 7, 20122 Milano, Italy

(Received November 15, 2006)

The Ring Imaging Cherenkov system of the LHCb experiment is presented, with particular emphasis on the status of the project.

PACS numbers: 29.40.Ka

1. Introduction

In one year from now, CERN's Large Hadron Collider will start delivering the first colliding proton beams. The LHCb collaboration [1] aims to fully exploit the LHC potential in the b-quark sector, spanning from CP violating phenomena to rare decays. The precision of these measurements will be high enough for contributions from TeV-scale New Physics to become accessible to experimental validation.

In order for this program to be pursued as extensively as possible, the LHCb detector has been designed to properly identify the decay products of b-hadrons. Particularly challenging is the positive identification of K mesons in the momentum range 1–100 GeV/c, relevant for B physics at the LHC. Two Ring Imaging Cherenkov detectors with three radiators constitute the core of the particle identification system of LHCb. Fig. 1 shows the essential contribution of particle identification to reduce background in a sample of $B_s^0 \to K^+K^-$ decays.

* Presented at the "Physics at LHC" Conference, Kraków, Poland, July 3–8, 2006.

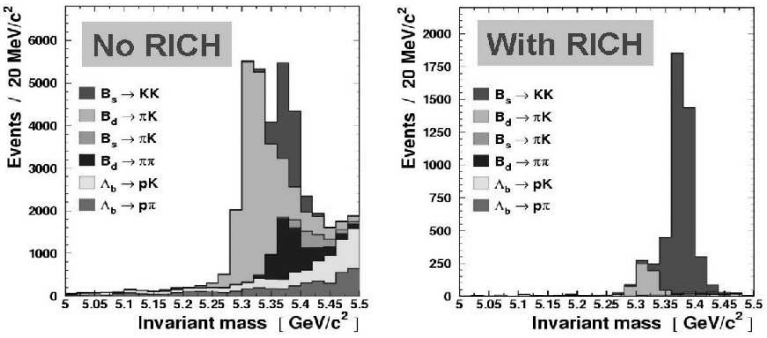

Fig. 1. Left: reconstructed invariant mass spectrum of $B_s^0 \to K^+K^-$ candidates before any particle identification is applied. Right: the same, but with particle identification criteria.

2. RICH 1

A schematic view of the RICH 1 detector [2, 3] is shown in Fig. 2. The detector optics is symmetric about the horizontal axis, with two sets of spherical and plane mirrors focusing the Cherenkov photons onto two photon detector arrays. Two Cherenkov radiators provide suitable refractive indices to cover the lower momentum range of interest for LHCb: solid silica aerogel for particles of momentum from 1 to 10 GeV/c and C_4F_{10} gas for momenta up to 65 GeV/c.

A substantial effort has been placed into the aerogel manufacturing process to achieve a material with unprecedented optical quality and world-record tile size. In 2004, the first sample of the final aerogel production has

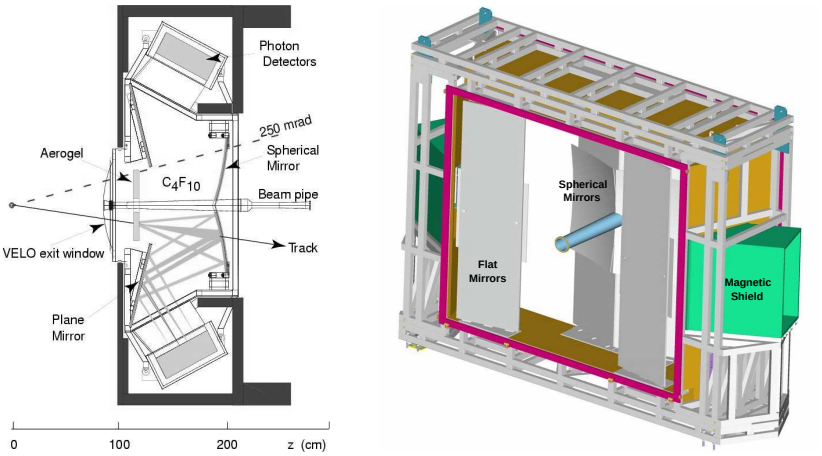

Fig. 2. Schematic of RICH1 (left) and RICH2 (right).

been verified for refractive index homogeneity by means of an electron beam and a table-top RICH detector [4]. Aerogel samples have also been exposed to several radiation sources to investigate possible degradations induced by the high particle flux expected during operation. Protons, neutron and γ irradiation, with fluxes several times higher than expected over the lifetime of the experiment, did not result in a measurable degradation of the optical properties of aerogel [5].

Another technological challenge of the RICH 1 detector is the spherical mirror system. It is placed inside the acceptance of the experiment. The fraction of radiation length X_0 and nuclear interaction length λ_{I} must, therefore, be minimised, and at the same time safeguarding the mechanical integrity of the optics. An industrial carbon fibre based composite mirror has been chosen as the best compromise between cost, optical quality, stability and material budget. A prototype of the RICH 1 spherical mirrors has been delivered early in 2006 and it has passed all relevant acceptance criteria and compatibility tests with respect to ionising radiation and fluorocarbon environment. The production and testing of the flat mirrors has been successfully completed.

Magnetic shielding surrounding the photon detectors in RICH 1 is crucial to reduce the stray field of the LHCb dipole magnet. The shielding also keeps the field integral between the vertex detector and the first tracking station high enough to be useful for the trigger [3].

The gas enclosure of RICH 1 has been manufactured and tested for gas leak tightness and mechanical precision. It provides confinement of the C_4F_{10} gas radiator as well as mechanical support and reference for the flat and spherical mirror arrays, the aerogel radiator frame, the laser system for alignment checks and the magnetic distortions monitoring device. It also houses the interfaces to the VELO seal and the beryllium beam pipe.

3. RICH 2

A schematic view of the RICH 2 detector [2] is also shown in Fig. 2. The detector is in a very advanced state. The superstructure has been assembled together with the carbon fibre–polymeric foam entrance window and the aluminium skin–polymeric foam exit window. The magnetic shielding for the photon detectors, mounted on each side of the superstructure, has been mapped in the LHCb magnetic field.

RICH 2 has 56 spherical and 40 flat mirrors which have been installed and aligned in a clean room. The mirror alignment has been verified after the transport and installation of RICH 2 in LHCb. No significant misalignment has been detected. The estimated contribution from the mirror system to the single photon Cherenkov angle uncertainty is of the order of 0.1 mrad.

4. The Hybrid Photon Detectors

The need for a fast and efficient photon detector operating at the LHC speed of 40 MHz with a very high (63%) active surface fraction and a good spatial resolution, lead to the development of a custom device, the pixel Hybrid Photon Detector (HPD) [6]. The HPD, designed and built in collaboration with industry, is shown schematically in Fig. 3. It consists of a 83 mm diameter vacuum tube with a quartz entrance window. The inner surface of the window is coated with a multilayer S-20 photocathode, biased at a -20 kV potential with respect to the anode, a pixelised silicon sensor. Two intermediate electrodes, one at -19.7 kV close to the cathode and the second, which is part of the tube body, at -16 kV, define the cross-focusing electron optics and a demagnification factor of 5. The anode contains 8192 pixels each of area 500 μm $\times$ 62.5 μm, actively OR-ed by the readout electronics in clusters of eight to form 1024 square super-pixels. This gives an effective granularity at the entrance window of 2.5×2.5 mm^2. An encapsulated 40 MHz chip is bump-bonded to the silicon anode. The chip performs the shaping and digitisation of the signal, which is then routed out of the HPD envelope. Arrays of 196 HPDs (RICH 1) and 288 HPDs (RICH 2) are arranged in columns which also host the electronics, shown in Fig. 3.

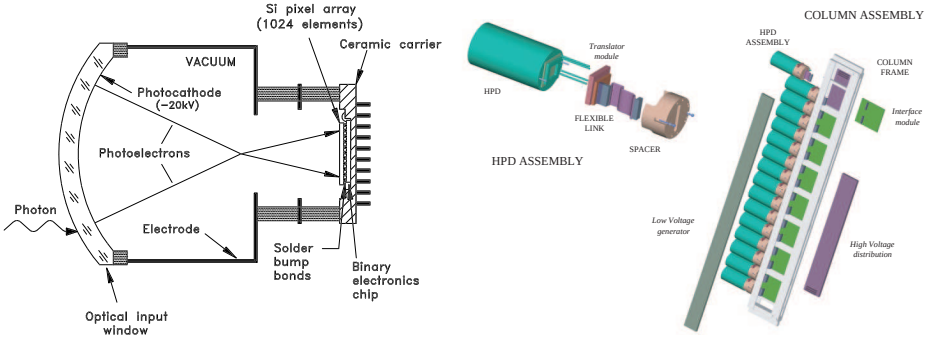

Fig. 3. Schematic of an HPD (left) and mounting scheme and mechanics (right).

The first beam test with production HPDs, power distribution boards and external readout (L0) boards has been carried out at the Frascati Beam Test Facility [7]. A total of 36 photon detectors mounted on production RICH 2 columns, shown in Fig. 4, detected Cherenkov photons emitted by the 500 MeV electrons passing through a Cherenkov gas volume.

Data have been collected with N_2 as Cherenkov radiator to test individual HPDs and time-align the L0 electronics with the asynchronous beam trigger signal. Runs with C_4F_{10} radiator have been also taken, giving a larger emission angle, which allows the detection of Cherenkov photons on up to four HPDs spanning three columns. A display showing Cherenkov rings

summed over many events, where the rings are distributed over four HPDs on two columns is shown in Fig. 4. The background level of the remaining HPDs is very low.

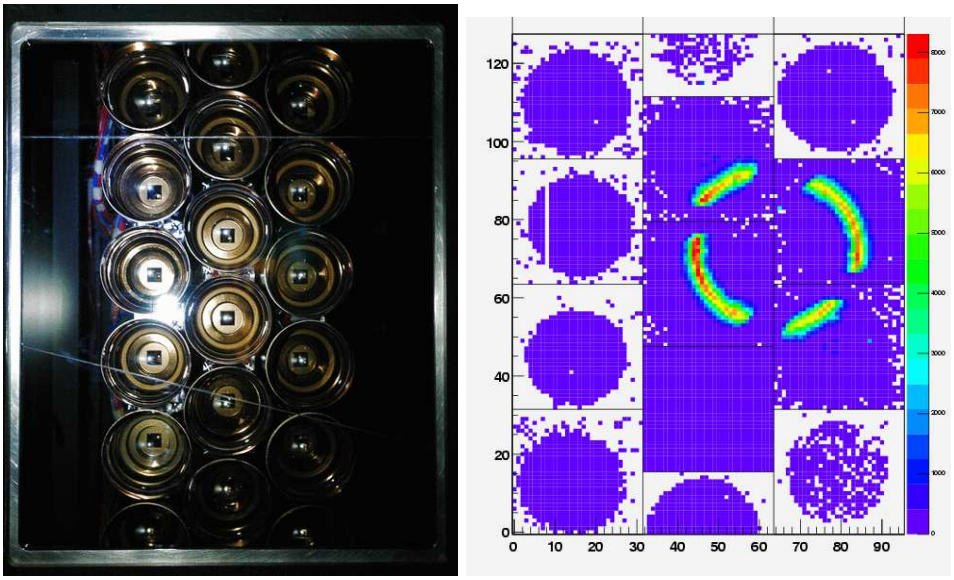

Fig. 4. Left: three columns of HPDs, taken from inside the testbeam gas enclosure. Right: an event display for a run with C_4F_{10} gas radiator. The Cherenkov photons emitted by 500 MeV electrons at the BTF facility are focussed onto four HPDs.

Extensive tests have been carried out in order to study the effect of the magnetic field inside the photon detector magnetic shielding. For fields higher than 10 Gauss, a fraction of photoelectrons are drifted out of the sensitive area of the anode by the Lorentz force. As a result, all HPDs will be surrounded by individual high magnetic permeability cylinders which restore almost field-free conditions in the path of photoelectrons. The residual field is still high enough to cause a distortion of the mapping of the photocathode onto the anode. A system based on the projection of a well-defined pattern onto the photon detectors is integrated inside RICH 1 and RICH 2 to allow a periodical correction of the magnetic distortions.

Operation of the HPD at high voltage requires great care in arranging power routing and insulation. The high voltage distribution boards are embedded in silicone rubber to guarantee no voltage leakage onto the column mechanical frame. A reliable insulation scheme based on Kapton has been identified which fits in the ~ 0.5 mm gap between the -20 kV HPD casing and the grounded magnetic shield.

The production of 484 HPDs required for the experiment is more than half way through. Two test stations have been set up for qualification of the photon detectors at the rate of 15 HPDs per station per month. The quality of the detectors is excellent, with a peak quantum efficiency $\sim 27\%$ and a rejection rate of only $\sim 3\%$.

5. Conclusions

The LHCb RICH project is in an advanced state. The construction of the RICH 2 detector is complete and the optics systems are mounted and aligned. RICH 2 is already placed in its final position in the experimental cavern. The columnwise modular mounting mechanics for the photon detectors has been manufactured and its population with HPDs, magnetic shields, readout and power distribution boards is ongoing. The RICH 1 gas enclosure has been manufactured, leak tested and recently installed in its final position. The carbon fibre based spherical mirrors are being manufactured and the complete production is expected to be finished by December 2006. The production of the photon detectors is about half-way complete and the quality is excellent.

REFERENCES

[1] The LHCb Collaboration, CERN/LHCC/98-4, Geneva, 1998.
[2] The LHCb Collaboration, CERN/LHCC/2000-037, Geneva, 2000.
[3] The LHCb Collaboration, CERN/LHCC/2003-030, Geneva, 2003.
[4] T. Bellunato *et al., Nucl. Instrum. Methods* **A556**, 140 (2006).
[5] T. Bellunato *et al., Nucl. Instrum. Methods* **A527**, 319 (2004).
[6] M. Moritz *et al., IEEE Trans. Nucl. Sci.* **51**, 1060 (2004).
[7] G. Mazzitelli *et al., Nucl. Instrum. Methods* **A515**, 524 (2003).